UNCLASSIFIED

AD 149456

Armed Services Technical Information Agency

ARLINGTON HALL STATION
ARLINGTON 12 VIRGINIA

FOR
MICRO-CARD
CONTROL ONLY

1 OF 1

NOTICE: WHEN GOVERNMENT OR OTHER DRAWINGS, SPECIFICATIONS OR OTHER DATA ARE USED FOR ANY PURPOSE OTHER THAN IN CONNECTION WITH A DEFINITELY RELATED GOVERNMENT PROCUREMENT OPERATION, THE U. S. GOVERNMENT THEREBY INCURS NO RESPONSIBILITY, NOR ANY OBLIGATION WHATSOEVER; AND THE FACT THAT THE GOVERNMENT MAY HAVE FORMULATED, FURNISHED, OR IN ANY WAY SUPPLIED THE SAID DRAWINGS, SPECIFICATIONS, OR OTHER DATA IS NOT TO BE REGARDED BY IMPLICATION OR OTHERWISE AS IN ANY MANNER LICENSING THE HOLDER OR ANY OTHER PERSON OR CORPORATION, OR CONVEYING ANY RIGHTS OR PERMISSION TO MANUFACTURE, USE OR SELL ANY PATENTED INVENTION THAT MAY IN ANY WAY BE RELATED THERETO.

UNCLASSIFIED

McLean Report No. E-114

GUST LOADS ON AIRSHIP FINS

Final Report

for the

Bureau of Aeronautics

Department of the Navy

Contract No. NOas 56-795-c

June, 1957

Prepared by: H. I. Flomenhoft

H. I. Flomenhoft

Approved by: R. E. Kemelhor

R. E. Kemelhor

Chief Engineer

TABLE OF CONTENTS

INTRODUCTION

The analysis of loads imposed on airplanes due to gusts and the establishment of applicable design criteria has had a long and complex history. Simplifications that were made during the middle 1930's led to the use of the "sharp-edge-gust formula" and an "effective gust velocity" based on the response of a standard airplane. After World War II it was evident that this concept was becoming obsolete, particularly with the advent and widespread use of techniques for analyzing the dynamic response of specific designs to actual loading conditions. This required a definition of "true" gust velocities and shapes for use in such analyses. Such a definition was accomplished several years ago. A thorough description of the history leading to the change and the basis of current methods of analysis is given in references (a) and (b). These reports list almost every pertinent reference in the field of gust-loads analysis. References (c), (d), and (e) are also of interest. Gust loading conditions for airplanes now specified in Bureau of Aeronautics Specification MIL-A-8629(Aer), reference (f), are based on the new method described in reference (a).

The determination of gust loads on airship fins has also made use of the effective sharp-edge-gust concept, with values of design gust velocity chosen more or less arbitrarily from airplane experience and model tests. It has become of interest to apply the new methods, which were developed for airplanes, to the analysis of airship fin loads caused by gusts. Therefore, the purpose of this study is to determine the response of airships subjected to gusts, considering the airship as a two-degree-of-freedom system and considering the lift-lag effects on the aerodynamic forces induced in the fins. Various primary parameters are varied to determine the significance of their effects. Also, the effects on the hull of gusts that are critical for the fins was investigated.

DEFINITION OF SYMBOLS

Symbols are defined in the order in which introduced into the analysis.

F_h = aerodynamic force on hull

M_h = aerodynamic moment on hull

F_t = aerodynamic force on tail

M = mass of airship

I = moment of inertia of airship

k_2 = transverse apparent mass factor

k' = rotational apparent mass factor

r = radius of gyration of effective airship, $\sqrt{\frac{(1+k')I}{(1+k_2)M}}$

z = vertical translation of tail

$\bar{z}$ = vertical translation of hull c.g.

θ = pitching rotation of hull c.g.

l_t = distance from c.g. to aerodynamic center of tail surface (¼-chord point)

L_g = lift due to gust

L_m = lift due to disturbed motion of tail

ρ = air density

V = forward velocity

S = area of tail

m = slope-of-lift curve of tail based on aspect ratio including projected area across hull between fins.

w_g = variable gust velocity, normal to flight path

U = maximum gust velocity

$\psi(s)$ = unsteady-lift function giving the growth of lift on a finite-span surface subjected to a sharp-edge gust.

$\phi(s)$ = unsteady-lift function giving the growth of lift on a finite-span surface subjected to a sudden unit change of angle of attack

$dC_L/d\alpha$ = slope of curve of coefficient of lift for hull

$dC_m/d\alpha$ = slope of curve of coefficient of moment for hull

S_h = maximum cross-sectional area of hull

l_h = total length of hull

s = distance travelled in half-chord lengths, $\left(\frac{2Vt}{c}\right)$

t = time travelled

c = mean aerodynamic chord of tail fin

a = half the length of the hull

R = maximum radius of the hull

$A(s)$ = response to sharp-edge gust

$R(s)$ = response to gust of any arbitrary shape

K_g = gust factor, peak value of R(s)

METHOD OF ANALYSIS

A. Establishment of Equations of Motion -

The basic simplification that is made in this analysis is to separate the effect of the gust on the fins from its effect on the hull. Later it is shown that the effect on the hull is small enough to justify this assumption. One reason for this is that the spatial extent of gusts most critical for the fins is small relative to the length of the hull. However, changes in total lift and moment acting on the hull due to changes in angle of attack or yaw will be included.

The airship will be represented by a simplified system shown by the following sketch:

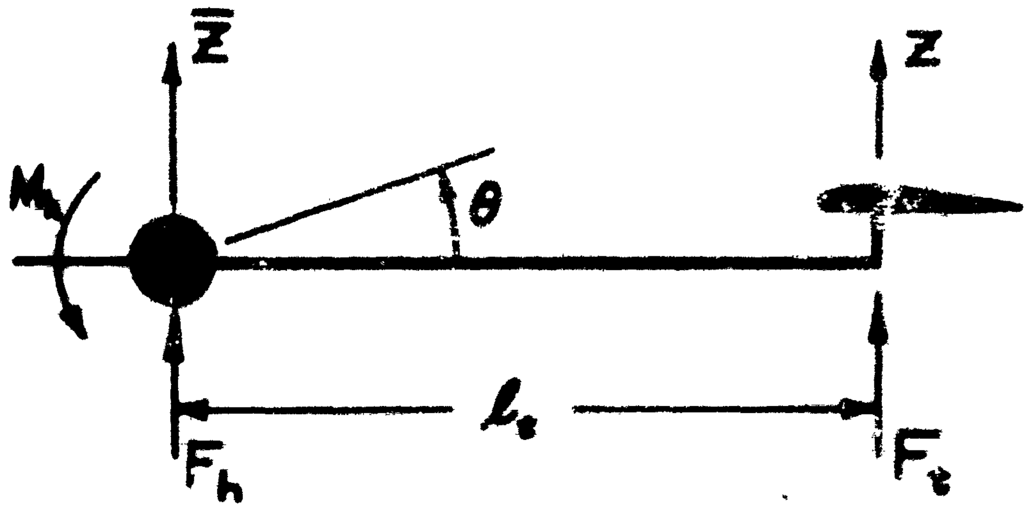

The coordinates of the hull c.g. are taken as $0, \bar{Z}$ and the coordinates of the tail are taken as ℓ_t, Z. The mass and moment of inertia of the lumped mass is taken to include the actual hull apparent mass factors. The aerodynamic behavior of the tail surface is assumed to be concentrated at the aerodynamic center. The gust is taken to act only on the fins.

The equations of motion for this system are:

$$F_h + F_t = M(1+k_1)\ddot{\bar{Z}} \tag{1}$$

$$M_h + F_t \ell_t = I(1+k')\ddot{\theta}$$

By geometry,

$$
\begin{aligned}
Z &= \bar{Z} + l_t \theta \\
\ddot{Z} &= \ddot{\bar{Z}} + l_t \ddot{\theta}
\end{aligned}
\qquad (2)
$$

Substituting (2) into (1), and eliminating $\ddot{\theta}$ from the first equation,

$$
\begin{aligned}
F_h + F_t &= (1+k_z)(M)\left(\ddot{\bar{z}} - \frac{F_t l_t^2}{(1+k')I} - \frac{M_h l_t}{(1+k')I}\right) \\
M_h + F_t l_t &= (1+k')I\ddot{\theta}
\end{aligned}
\qquad (3)
$$

Introducing the radius of gyration of the system, including apparent mass factors, the equations of motion can be reduced to

$$
\begin{aligned}
(1+k_z)M\ddot{\bar{z}} &= F_h + F_t\left(1+\frac{l_t^2}{r^2}\right) + M_h\frac{l_t}{r^2} \\
(1+k')I\ddot{\theta} &= M_h + F_t l_t
\end{aligned}
\qquad (4)
$$

It is now necessary to define the aerodynamic forces in these equations.

$$F_t = L_g + L_m$$

L_g = Lift due to the gust directly

L_m = Lift due to the disturbed motion of the tail caused by the gust

F_h = Lift on airship hull due to change in angle caused by the gust acting on the tail.

M_h = Moment on airship hull due to change in angle caused by the gust acting on the tail.

Prior to encountering the gust, the airship is assumed to be in equilibrium. Angular changes due to the gust are measured from the initial position, which can therefore be taken to be zero. L_g and L_m must be determined by introducing appropriate lift-lag functions into Duhamel integrals in order to determine the accumulated lift at any time while the angle of attack is varying. Further background on this step is given in reference (c), pages 262-265.

$$L_g = \frac{1}{2}\rho V^2 S m \int_0^s \psi'(s-\sigma)\frac{w_g}{V}(\sigma)\,d\sigma$$

$$L_m = -\frac{1}{2}\rho V^2 S m \int_0^s \phi(s-\sigma)\frac{d}{d\sigma}\left[\theta(\sigma) + \frac{\dot{z}(t)}{V}\right]d\sigma \tag{5}$$

$$F_h = C_L \frac{1}{2}\rho V^2 S_h = \frac{dC_L}{d\alpha}\frac{1}{2}\rho V^2 S_h \theta(t)$$

$$M_h = C_m \frac{1}{2}\rho V^2 S_h \ell_h = \frac{dC_m}{d\alpha}\frac{1}{2}\rho V^2 S_h \ell_h \theta(t)$$

$\psi(s)$ and $\phi(s)$ are the respective functions which describe the build-up in lift and occurs on an airfoil penetrating a unit sharp-edge gust and an airfoil experiencing an instantaneous unit change in angle of attack. Putting all of these expressions for the aerodynamic forces into the equations of motion gives the following:

$$(1+k_z)M\ddot{z} = \frac{dC_L}{d\alpha}\frac{1}{2}\rho V^2 S_h \theta(t) + \frac{dC_m}{d\alpha}\frac{1}{2}\rho V^2 S_h \frac{\ell_h \ell_t}{r^2}\theta(t)$$
$$+\frac{1}{2}\rho V^2 S m\left(1+\frac{\ell_t^2}{r^2}\right)\left\{\int_0^s \psi'(s-\sigma)\frac{w_g(\sigma)}{V}d\sigma\right.$$
$$\left.-\int_0^s \phi(s-\sigma)\frac{d}{d\sigma}\left[\theta(\sigma) + \frac{\dot{z}(t)}{V}\right]d\sigma\right\} \tag{6}$$

$$(1+k')I\ddot{\theta} = \frac{dC_m}{d\alpha}\frac{1}{2}\rho V^2 S_h \ell_h \theta(t)$$
$$+\frac{1}{2}\rho V^2 S m \ell_t\left\{\int_0^s \psi'(s-\sigma)\frac{w_g(\sigma)}{V}d\sigma\right.$$
$$\left.-\int_0^s \phi(s-\sigma)\frac{d}{d\sigma}\left[\theta(\sigma) + \frac{\dot{z}(t)}{V}\right]d\sigma\right\}$$

Since the lift-growth functions depend on the distance rather than the time travelled, the equations of motion are transformed to make distance the independent variable.

Let $s = \left(\frac{2V}{c}\right)t$, the distance travelled in half-chords of the fin.

$$ds = \left(\frac{2V}{c}\right)dt$$

$$\dot{z} = \frac{dz}{dt} = \frac{dz}{ds}\cdot\frac{ds}{dt} = z'\left(\frac{2V}{c}\right)$$

$$\ddot{z} = z''\left(\frac{2V}{c}\right)^2 \qquad (7)$$

Similarly,

$$\dot{\theta} = \theta'\left(\frac{2V}{c}\right)$$

$$\ddot{\theta} = \theta''\left(\frac{2V}{c}\right)^2$$

Putting these expressions into the equations of motion, solving for z" and θ", and simplifying,

$$\begin{aligned} z''(s) = {} & \frac{dC_L}{d\alpha}\frac{1}{2}\rho S_h \frac{c^2}{4}\frac{\theta(s)}{(1+k_z)M} + \frac{dC_m}{d\alpha}\frac{1}{2}\rho S_h \frac{\ell_h \ell_t}{r^2}\frac{c^2}{4}\frac{\theta(s)}{(1+k_z)M} \\ & + \frac{1}{2}\rho S m\left(1+\frac{\ell_t^2}{r^2}\right)\frac{c^2}{4}\frac{1}{(1+k_z)M}\left\{\int_0^s \psi'(s-\sigma)\frac{w_g(\sigma)}{V}d\sigma \right. \qquad (8) \\ & \left. - \int_0^s \phi(s-\sigma)\frac{d}{d\sigma}\left[\theta(\sigma) + \frac{2}{c}z'(\sigma)\right]d\sigma \right\} \end{aligned}$$

$$\theta''(s) = \frac{dC_m}{d\alpha}\frac{1}{2}\rho S_h \ell_h \frac{c^2}{4}\frac{\theta(s)}{(1+k')I}$$
$$+ \frac{1}{2}\rho S m \ell_t \frac{c^2}{4}\frac{1}{(1+k')I}\left\{\int_0^s \psi'(s-\sigma)\frac{w_g(\sigma)}{V}d\sigma \right. \qquad (8)$$
$$\left. - \int_0^s \phi(s-\sigma)\frac{d}{d\sigma}\left[\theta(\sigma) + \frac{2}{c}z'(\sigma)\right]d\sigma\right\}$$

Constants can now be defined as follows:

$$K_1' = \frac{c}{4\mu_h} \qquad \mu_h = \frac{2(1+k_2)M/S_h}{\rho c \; dC_L/d\alpha}$$
$$K_1 = K_1' + K_2\ell_t \qquad \nu_h = \frac{2(1+k_2)M/S_h}{\rho c \; dC_m/d\alpha} \qquad (9)$$
$$K_2 = \frac{c}{4\nu_h}\cdot\frac{\ell_h}{r^2}$$
$$K_3 = \frac{c}{4\mu_e} \qquad \mu_e = \frac{2(1+k_2)M/S}{\left(1+\frac{\ell_t^2}{r^2}\right)\rho c m}$$
$$K_4 = \frac{c}{4\mu}\cdot\frac{\ell_t}{r^2} \qquad \mu = \frac{2(1+k_2)M/S}{\rho c m}$$

Using these constants, the equations of motion can now be stated more simply in the following manner:

$$Z''(s) = K_1\theta(s) + K_3\left\{\int_0^s \psi'(s-\sigma)\frac{w_g(\sigma)}{V}d\sigma - \int_0^s \phi(s-\sigma)\frac{d}{d\sigma}\left[\theta(\sigma) + \frac{2}{c}z'(\sigma)\right]d\sigma\right\}$$

$$(10)$$

$$\theta''(s) = K_2\theta(s) + K_4\left\{\int_0^s \psi'(s-\sigma)\frac{w_g(\sigma)}{V}d\sigma - \int_0^s \phi(s-\sigma)\frac{d}{d\sigma}\left[\theta(\sigma) + \frac{2}{c}z'(\sigma)\right]d\sigma\right\}$$

THESE TWO EQUATIONS REPRESENT THE BASIC MATHEMATICAL STATEMENT OF THE "STICK-FIXED" CONDITION OF THE AIRSHIP ENCOUNTERING A GUST.

Certain simplifying assumptions can be made to expedite solution of these equations. First, consider only the terms with the braces. In the first integral, let $w_g(\sigma) = U$, a constant, or sharp-edge gust. Solutions obtained for a sharp-edge gust can be used to obtain a response for any gust profile, using the Duhamel integral. In the second integral, $\phi(s-\sigma)$ can be assumed to be unity since the aspect ratio of airship tail surfaces is generally very low. This means that the initial lift due to an instantaneous change in angle of attack is about 70% of the steady-state lift, to which it converges in less than three chord lengths. With these assumptions, the integrals are treated as follows:

$$\int_0^s \psi'(s-\sigma)\frac{w_g(\sigma)}{V}\,d\sigma = \frac{U}{V}\int_0^s \psi'(s-\sigma)\,d\sigma = \frac{U}{V}\,\psi(s)$$

$$\int_0^s \phi(s-\sigma)\frac{d}{d\sigma}\left[\theta(\sigma) + \frac{2}{c}z'(\sigma)\right]d\sigma = \theta(s) + \frac{2}{c}z'(s) \tag{11}$$

Equations (10) therefore become

$$z''(s) = K_1\,\theta(s) + K_3\left[\frac{U}{V}\psi(s) - \theta(s) - \frac{2}{c}z'(s)\right]$$

$$\theta''(s) = K_2\,\theta(s) + K_4\left[\frac{U}{V}\psi(s) - \theta(s) - \frac{2}{c}z'(s)\right] \tag{12}$$

The equations of motion are now in a suitable form for solution, but before proceeding with this, the next section will establish the function $\psi(s)$ that will be used.

3. Unsteady-lift Functions -

The exact form of the lift-growth functions for an airfoil subjected to sudden changes in angle of attack or penetrating gusts is dependent on the aspect ratio. Extending previous work by Wagner and Kussner on the infinite-aspect-ratio wing, Jones solved the problem for the finite-aspect-ratio wing in reference (g). Figure 1 was prepared from data given in reference (g) for aspect ratios of 3, 6, and infinity. The limiting case for an aspect ratio

of zero is shown by the empirical dotted curve, wherein the lag effect is considered to be due only to the penetration of the full chord length. The function $\psi(s) = 1 - e^{-s}$ was selected as a simple approximation applicable to the range of aspect ratios from 1 to 2. This simple form of the function facilitates numerical solution of the equations later.

C. Solution of Equations -

The equations of motion are now in a form that can be readily solved by use of the Laplace Transform. While it is possible to solve the differential equations directly for $z(s)$, it is much easier to solve for $z''(s)$ directly and then integrate numerically to obtain $z'(s)$ and $z(s)$. Referring to pages 14, 294, and 295 of reference (h), the following operations can be written:

$$\mathcal{L}\{z''(s)\} = \bar{z}''(p) \qquad \mathcal{L}\{\theta''(s)\} = \bar{\theta}''(p)$$

$$\mathcal{L}\{z'(s)\} = \frac{1}{p}\bar{z}''(p) \qquad \mathcal{L}\{\theta'(s)\} = \frac{1}{p}\bar{\theta}''(p)$$

$$\mathcal{L}\{z(s)\} = \frac{1}{p^2}\bar{z}''(p) \qquad \mathcal{L}\{\theta(s)\} = \frac{1}{p^2}\bar{\theta}''(p) \tag{13}$$

$$\mathcal{L}\{\psi(s)\} = \mathcal{L}\{1 - e^{-s}\} = \frac{1}{p} - \frac{1}{p+1} = \frac{1}{p(p+1)}$$

Introducing these transforms into equation (12) leads to the following algebraic simultaneous equations:

$$\bar{z}''(p) = \frac{K_1 - K_2}{p^2}\bar{\theta}''(p) + K_3\left[\frac{U}{V}\left(\frac{1}{p(p+1)}\right) - \frac{2}{pc}\bar{z}''(p)\right]$$

(14)

$$\bar{\theta}''(p) = \frac{K_2 - K_4}{p^2}\bar{\theta}''(p) + K_4\left[\frac{U}{V}\left(\frac{1}{p(p+1)}\right) - \frac{2}{pc}\bar{z}''(p)\right]$$

Collect $\bar{z}''(p)$ and $\bar{\theta}''(p)$ terms,

$$\left[1 + \frac{2K_3}{pc}\right]\bar{Z}''(p) - \frac{K_1 - K_3}{p^2}\,\bar{\theta}''(p) = \frac{K_3 U}{V}\left(\frac{1}{p(p+1)}\right)$$

$$\frac{2K_4}{pc}\,\bar{Z}''(p) + \left[1 - \frac{K_2 - K_4}{p^2}\right]\bar{\theta}''(p) = \frac{K_4 U}{V}\left(\frac{1}{p(p+1)}\right) \tag{15}$$

Eliminating $\bar{\theta}''(p)$ and solving for $\bar{z}''(p)$,

$$\bar{Z}''(p) = K_3\frac{U}{V}\left\{\frac{p^2 + \frac{1}{K_3}(K_1K_4 - K_2K_3)}{\left[p^3 + \frac{2K_3}{c}p^2 + (K_4 - K_2)p + \frac{2}{c}(K_1K_4 - K_2K_3)\right](p+1)}\right\} \tag{16}$$

Let N(p) and Q(p) functions be defined as follows:

$$N(p) = p^2 + M_2/M_1$$

$$Q(p) = (p^3 + M_3p^2 + M_4p + M_5)(p+1) \tag{17}$$

where

$$M_1 = K_3$$
$$M_2 = K_1K_4 - K_2K_3$$
$$M_3 = \frac{2K_3}{c} \tag{18}$$
$$M_4 = K_4 - K_2$$
$$M_5 = \frac{2}{c}M_2$$

If the polynomial Q(p) is now assumed to be completely factored, it will appear in the form

$$Q(p) = (p - B_1)(p - B_2)(p - B_3)(p+1) \tag{19}$$

Using Heaviside's Partial Fractions Expansion (see Section 16 of reference (h)), the inverse transform can be readily obtained, so that the solution for $z''(s)$ can be stated in the form,

$$Z''(s) = K_3 \frac{U}{V} \left\{ \frac{N(B_1)}{Q_1(B_1)} e^{B_1 s} + \frac{N(B_2)}{Q_2(B_2)} e^{B_2 s} + \frac{N(B_3)}{Q_3(B_3)} e^{B_3 s} + \frac{N(1)}{Q_4(1)} e^{-s} \right\} \quad (20)$$

In this form it must be noted that $Q_n\ (B_n)$ is defined as the number (which may be complex) resulting from substituting $p = B_n$ into all the factors of $Q(p)$, but omitting the factor $(p - B_n)$, which is zero.

The solution for $\theta''(s)$ can be obtained in a similar manner, but is not carried through here because $z''(s)$ is the pertinent variable that determines the structural loads acting on the airship fins. The solution for $z''(s)$ can be put into non-dimensional form by dividing by the simple solution that would be obtained if lift-lag effects were neglected and the fins were assumed constrained from moving in the direction of the gust.

$$\text{Acceleration} = \frac{\text{"Constrained-fin" force}}{\text{Effective mass}} = \frac{\frac{1}{2} \rho V^2 S m \,U/V}{\dfrac{W(1+k_2)}{g\left(1+\frac{k^2}{r^2}\right)}}$$

Transforming $\ddot{Z}(t)$ to $z''(s)$ requires multiplying by $\left(\frac{c}{2V}\right)^2$, and dividing all of this into equation (20) gives the non-dimensional response factor to a sharp-edge gust.

$$A(s) = \frac{K_3\, U/V}{\dfrac{\frac{1}{2} \rho V^2 S m\, U/V \left(\frac{c^2}{4V^2}\right)}{\dfrac{W(1+k_2)}{g\left(1+\frac{k^2}{r^2}\right)}}} \sum_{i=1}^{4} \frac{N(B_i)}{Q_i(B_i)} e^{a_i s} = \sum_{i=1}^{4} \frac{N(B_i)}{Q_i(B_i)} e^{a_i s}$$

All of the factors outside the summation cancel nicely to unity, leaving only the summation as the non-dimensional response factor, $A(s)$. With this factor the response to any gust can now be obtained using the Duhamel integral.

$$R(s) = \int_0^s w_g'(\sigma)\, A(s-\sigma)\, d\sigma$$

where $w_g'(s)$ is the derivative of the gust velocity distribution. The 1 - cosine gust will be used in the following form:

$$w_g(s) = \frac{U}{2}\left(1 - \cos\frac{2\pi s}{L}\right)$$

$$w_g'(s) = \frac{\pi U}{L} \sin\frac{2\pi s}{L}$$

Substituting this expression into the Duhamel integral yields,

$$R(s) = \frac{\pi U}{L} \int_0^s \sin\frac{2\pi\sigma}{L}\, A(s-\sigma)\, d\sigma$$

This is readily solved by numerical integration. The calculating procedure is explained in the numerical example of a typical case given in Appendix A.

D. Parameters -

The basic parameters involved in the solution of this problem are given by equations (9) and are restated here.

$$K_1' = \frac{c}{4\mu_h} \qquad \mu_h = \frac{2(1+k_z)M/S_h}{\rho c\, dC_L/d\alpha}$$

$$K_1 = K_1' + K_2 l_t \qquad \nu_h = \frac{2(1+k_z)M/S_h}{\rho c\, dC_m/d\alpha}$$

$$K_2 = \frac{c}{4\nu_h} \cdot \frac{l_t}{r^2} \qquad \mu_e = \frac{2(1+k_z)M/S}{\left(1+\frac{l_t^2}{r^2}\right)\rho c m}$$

$$K_3 = \frac{c}{4\mu_e}$$

$$K_4 = \frac{c}{4\mu} \cdot \frac{l_t}{r^2} \qquad \mu = \frac{2(1+k_x)M/S}{\rho c m}$$

Data was obtained from the Bureau of Aeronautics for a representative group of airships. Values for apparent mass factor, when none were given, were taken from Figure 2, based on Art. 155 of reference (i).

In order to obtain values for $dC_L/d\alpha$ and $dC_m/d\alpha$ for the airship hulls, aerodynamic data available for bodies of revolution in references (j), (k), (l), and (m) were analyzed. Figure 3 presents curves of C_L versus α for various fineness ratios. Values of C_L, based on maximum cross-sectional area, are seen to be roughly in proportion to the fineness ratio, or, in other words, the total value of lift is roughly proportional to the planform area. Although the correlation is not considered especially good, it is shown later that the effect of aerodynamic terms is quite small and it therefore suffices to take average values based on Figure 3. Also, linear approximations to these curves were taken by using the secant values through $\alpha = 0$ and 10°. Based on the available data, $dC_L/d\alpha$ was taken as 0.019/degree for a fineness ratio of 4.24. In a similar manner, $dC_m/d\alpha$ was taken to be 0.003/degree for a fineness ratio of 4.24. For other fineness ratios, these values were adjusted proportionately.

Values of the basic parameters r motions in the X-Z plane are listed in the following table for four different types of airships:

AIRSHIP	ZSG-4	ZS2G-1	ZPG-2	ZR-3 (Los Angeles)
Fin Arrangement	+	⅄	×	+
μ_h	19.4	14.5	17.8	13.7
ν_h	122.9	91.7	112.8	86.8
μ_e	5.63	5.44	5.60	7.26
μ	22.8	21.4	27.4	40.0
K_1	1.06	1.97	1.64	3.31
K_2	.00629	.0110	.00750	.00740
K_3	1.68	2.28	2.04	2.34
K_4	.0123	.0168	.0122	.00686

NOTE: Forces on the tail and, therefore, the above parameters are based on the exposed area of the fins.

The values given in this table and certain variations of them were used in computing a series of numerical examples to illustrate the effects of gusts and the importance of different parameters.

DISCUSSION

Using the method of analysis and parameters presented in the previous section, a series of numerical examples were computed. The first objective was to determine the basic nature of the airship response and the size of gust which produced maximum peak accelerations. The ZSG-4 airship was used for this purpose. The calculated response to a sharp-edge gust is shown in Figure 4; this was used to compute peak acceleration responses to 1 - cosine gusts of various lengths. These results are shown in Figure 5 and indicate that a gust with a total length of about six half-chords can be taken as critical, that is, the shortest-length gust near peak response. A time history of response to this gust is shown in Figure 6. The significant result shown by these curves is that peak acceleration occurs very shortly after the gust peak, which, for a typical forward speed of 52.5 knots (chosen to give an even time scale), is of the order of 0.4 seconds from the beginning of any perceptible displacement or motion of the fins. It therefore appears that there cannot be any significant pilot response at the time of peak acceleration caused by the gust. After a second has elapsed, however, velocities and displacements become very large, and it is certain that pilot response will begin to affect the airship motions at this stage.

Also shown on Figure 6 is the response calculated with the hull aerodynamic terms entirely omitted. It is evident that the effect of this change is very small, and justifies the linear approximations developed previously for $dC_L/d\alpha$ and $dC_m/d\alpha$. It would really be justified to omit them in all remaining analyses, but they were included because it involved virtually no additional effort in the computations.

The next objective to the program was to ascertain the extent to which the airship was affected by the action of the gust directly on the hull. The method of analysis for this condition is described in Appendix B. Results are shown on Figure 7 for the ZS2G-1 airship for repeated and isolated gusts equivalent to the three-chord-length gusts found to be critical for the fins, and for six-chord-length gusts. The curves shown are based on a true gust velocity of 50 feet per second. It is evident that the pitch angle caused by the gust travelling over the length of the hull is small. The case of greatest interest, the isolated 2.5-chord sinusoidal gust, produces a pitch angle of about 1.6 degrees. The fin is therefore subjected to an increment of load

due to this pitch angle in addition to the angle of attack induced directly by the gust. This latter angle is of the order of 20 degrees for a 50 foot-per-second gust, so that the effect of the gust on the hull is less than 10 percent. A gust of twice the length produces angles up to 2.8 degrees, but this will be offset to some degree by the lower fin response and the effect of pilot correction. The effect of the gust on the hull is therefore seen to be significant enough to be considered in any refined analysis of a specific design, but is small enough to justify the original assumption that the effect of the gust on the fins can be treated independent of the hull. For overall design criteria, this effect could be reasonably taken into account by choosing a design gust velocity about 10% higher than the actual limit considered applicable.

The third and primary objective to the program was to determine the significance of the various airship parameters. In particular, it is of interest to establish whether or not the parameter μ_e can be considered the basic one, since it is directly analogous to the airplane mass parameter that establishes airplane response to gusts. This point is actually somewhat academic, since airships are all so similar in general design that there is not much variation in the parameters. However, in order to see the effect of a radical change in μ_e, three numerical examples were computed starting with the basic characteristics of the ZS2G-1 airship. In the first example, the moment of inertia was arbitrarily increased tenfold; in the second example, the moment of inertia was restored to normal and the fin area was reduced to produce the same μ_e; in the third example, the mass was increased to produce the same μ_e. Moment of inertia appears in the parameter μ_e only, fin area appears in μ_e and μ, and mass appears in all four parameters, μ_h, ν_h, μ_e, and μ. Therefore, this appears to cover the range of possible variations. Time histories of acceleration responses are shown on Figure 8.

Finally, the peak acceleration responses computed for the various cases are plotted as a function of μ_e in Figure 9. Also shown is the gust-factor curve for airplanes, as given in reference (f), for comparison. It can be seen that the behavior is similar, except that airship responses are higher because lift-lag effects for the low-aspect-ratio tail surfaces are less pronounced than for airplane wings. It is considered that Figure 9 could form the basis for a new design gust criterion for airship fins.

Some flight-test data from instrumented airships obtained by the Aeronautical Structures Laboratory, Naval Air Material Center, was investigated to see if there was any experimental verification of type of responses shown in this report. Unfortunately, the records available were intended for a different purpose, so that the relatively high-frequency loads caused by gust loads on the fins could not be detected. (See Figure 10) One thing that the records did bring out is that large amounts of control-surface deflection from one extreme to the other were constantly being applied. The airship is basically unstable and response to control application has such a lag that the pilot tends to apply control in discrete increments as soon as he detects a pitching velocity and then waits to see the effect. This means that full throw of the controls is often applied and held for periods as long as five seconds. In continuous turbulence this would certainly mean combinations of critical gust loads with maximum control position.

The control-surface motions appeared to be far more active than warranted by the fairly mild variations of pitch attitude. Close examination, however, revealed that control-surface motion was closely correlated with every detectable change in pitch attitude. Most of the pilot's work, therefore, is making corrections for small disturbances. This suggests that a gust-alleviating device could be quite promising as a means for improving flying qualities.

It would be of great value to obtain more data from instrumented airships flying in turbulent air. The instrumentation should be set up to detect and record the types of critical gusts indicated by the analysis. It is recommended that a conventional airplane such as the SNB also be instrumented and flown along with the airship in turbulence. The airplane could make passes by the airship and record in intervals as it goes by. With this procedure, the airplane would serve as an independent means for checking the level of turbulence and correlating the results obtained from the airship.

CONCLUSIONS

1. Gusts that cause critical loading of airship fins are about three chord lengths long, using the idealized 1 - cosine gust shape. Peak loads occur when the fin has travelled between 1½ and 2 chord lengths from the point where the leading edge first strikes the gust.

2. The effective mass parameter of the airship fins is the most significant parameter for determining the response. The variation of peak acceleration response with effective mass parameter is similar to the variation of gust factor with airplane mass parameter, except that the responses are much greater. The effective mass parameter could be used as the basis for a gust design criterion, or, since airships are generally so similar, one value of gust factor could be selected as applicable to all cases.

3. Design gust conditions should be specified in combination with full throw of the control surface.

4. A flight-test program to obtain data on gust loads would be of value. Such a program should include measurement of accelerations at the tail with an oscillograph paper speed suitable for detecting gusts of about three fin chords in length. Measurement of turbulence in the same region as the airship, using an instrumented conventional airplane, would provide an independent check of the level of turbulence.

REFERENCES

(a) NACA Report 1206, "A Revised Gust-Load Formula and a Re-evaluation of V-g Data Taken on Civil Transport Airplanes from 1933 to 1950" by Kermit G. Pratt and Walter G. Walker, 1954.

(b) NACA Report 997, "Summary of Information Relating to Gust Loads on Airplanes", by Philip Donely, 1950.

(c) "An Investigation of Stresses in Aircraft Structures under Dynamic Loading" by R.L. Bisplinghoff, G. Isakson, T.H.H. Pian, H.I. Flomenhoft, and T.F. O'Brien dated January 21, 1949. MIT report to Bureau of Aeronautics, Contract No. NOa(s) 8790.

(d) "Gust Loads on Rigid and Elastic Airplanes" by R.L. Bisplinghoff, G. Isakson and T.F. O'Brien dated August 15, 1949. MIT report to Bureau of Aeronautics, Contract No. NOa(s) 8790.

(e) "A Further Study of Gust Loads on Rigid and Elastic Airplanes" by G. Isakson, C.W. Brenner, and T.F. O'Brien dated July 26, 1950. MIT report to Bureau of Aeronautics, Contract No. NOa(s) 8790.

(f) "Airplane Strength and Rigidity", Military Specification MIL-A-8629(Aer) dated 28 August 1953.

(g) NACA Report 681, "The Unsteady Lift of a Wing of Finite Aspect Ratio" by Robert T. Jones, 1940.

(h) "Modern Operational Mathematics in Engineering" by Ruel V. Churchill, McGraw-Hill Book Company, Inc., 1944.

(i) "Hydrodynamics" by H. Lamb, Cambridge University Press, Sixth Edition, 1932.

(j) "Performance of Airships" by K. Arnstein and W. Klemperer, Division R of "Aerodynamics Theory", Vol. VI, W.F. Durand, Julius Springer, Berlin, 1934.

(k) NACA Report 1048, "A Study of Effects of Viscosity on Flow over Slender Inclined Bodies of Revolution", by H. Julian Allen and Edward W. Perkins, 1951.

(l) NACA RM A51H22, "Lift, Drag, and Pitching Moment of Low-Aspect-Ratio Wings at Subsonic and Supersonic Speeds - Body of Revolution", by John C. Heitmeyer, October 1951.

(m) NACA Technical Report 1155, "A Comparison of Experimental Subsonic Pressure Distributions about Several Bodies of Revolution with Pressure Distributions Computed by Means of the Linearized Theory", by Clarence W. Matthews, 1953.

(n) "Modern Developments in Fluid Dynamics", by S. Goldstein; Axford, the Clarendon Press, 1938, vol. II.

APPENDIX A

NUMERICAL EXAMPLE: ZSG-4 AIRSHIP

$K_1 = 1.061$ $M_1 = K_3 =$ 1.578

$K_2 = 0.006286$ $M_2 = K_1K_4 - K_2K_3 =$ 0.003163

$K_3 = 1.578$ $M_3 = \frac{2}{C}K_3 =$ .08890

$K_4 = 0.01233$ $M_4 = K_4 - K_2 =$ 0.06044

$C = 35.5$ $M_5 = \frac{2}{C}M_2 =$ 0.0001782

$$N(p) = p^2 + M_2/M_1 = p^2 + 0.002004$$

$$Q(p) = (p^3 + M_3p^2 + M_4p + M_5)(p+1)$$

$$= (p^3 + .0889p^2 + .006044p + .0001782)(p+1)$$

Factoring first by trial and error to obtain the real root, and then by quadratic formula,

$$Q(p) = (p + .04380)(p + .02255 + .05967i)(p + .02255 - .05967i) \times (p+1)$$

$B_1 = -.04380$

$B_2 = -.02255 - .05967i$

$B_3 = -.02255 + .05967i$

$B_4 = -1$

$$N(B_1) = (-.0438)^2 + .002004 = .003922$$

$$Q_1(B_1) = (-.02125 + .05967i)(-.02125 - .05967i)(.9562) = .003836$$

$$\frac{N(B_1)}{Q_1(B_1)} = \frac{.003922}{.003836} = \underline{1.022}$$

$$N(B_2) = (-.02255 - .05967i)^2 + .002004 = -.001048 + .002691i$$

$$Q_2(B_2) = (.02125 - .05967i)(-.1193i)(.9774 - .05967i) = -.007112 - .002054i$$

$$\frac{N(B_2)}{Q_2(B_2)} = \frac{-.001048 + .002691i}{-.007112 - .002054i} = \underline{.03515 - .3885i}$$

$$\frac{N(B_3)}{Q_3(B_3)} \qquad \frac{N(B_2)}{Q_2(B_2)}$$

$$N(B_4) = (-1)^2 + .002004 = 1.002$$

$$Q_4(B_4) = (-.9562)(-.9774 + .05967i)(-.9774 - .05967i) = -.9170$$

$$\frac{N(B_4)}{Q_4(B_4)} = \frac{1.002}{-.9170} = \underline{-1.093}$$

$$A(s) = 1.022\,e^{-.04388s} + (.03515 - .3885i)\,e^{(-.02255 - .05967i)s} + (.03515 + .3885i)\,e^{(-.02255 + .05967i)s} - 1.093\,e^{-s}$$

$$A(s) = 1.022\,e^{-.04388s} - 1.093\,e^{-s} + e^{-.02255s}(.0705\cos\theta + .7771\sin\theta)$$

where $\theta = .05967(57.3)s = 3.419s$ degrees

This equation was used to compute and tabulate values of $A(s)$ from $s = 0$ to 10. Computation of the response to a 6-half-chord-length gust with a peak velocity of unity is based on the integral,

$$R(s) = \frac{\pi}{6}\int_0^s \sin\frac{2\pi\sigma}{6}\,A(s-\sigma)\,d\sigma$$

This was solved by numerical integration, trapezoidal rule, using $\Delta\sigma = .25$, for s = 0 to 8.

Therefore, $$R(n) = \frac{\pi}{24} \sum_{\sigma=0}^{n} \left(\sin \frac{\pi\sigma}{6}\right)\left(A(n-\sigma)\right)$$

wherein the first and last terms are zero.

The procedure for accomplishing this was to list values of A(s) at s = .25 intervals in reverse order, starting with the value of A(s) at s = 8 and ending with zero, the value at s = 0, at the bottom of the column. On another sheet, successive values of sin $\frac{\pi\sigma}{6}$ at σ = .25 intervals were listed from σ = 0 to 8 in a column with zero, the value at σ = 0, at the top. A succession of sums of products was then made by first placing the A(s) sheet so that the bottom value, zero, appeared alongside the top value, zero, of sin $\frac{\pi\sigma}{6}$. The product of the two adjacent numbers, zero, was recorded. The A(s) sheet was then moved down one number so that A(.25) appeared alongside the first value of sin $\frac{\pi\sigma}{6}$. The s of two products of adjacent numbers was then computed, which was still zero. Again the sheet was moved down to yield three pairs of adjacent numbers. Now the sum of products gives a finite value. As the sheet is moved down for each new summation, one additional product is picked up until 23 products (excluding the two zero terms) are involved at s = 6. Since this is the end of the gust, further values of sin $\frac{\pi\sigma}{6}$ are all zero and 23 products continue to be involved for values of R(s) beyond s = 6.

APPENDIX B

EFFECT OF GUST ACTING DIRECTLY ON HULL

The total loads imposed on airship fins by gusts must also include any angle of attack caused by the gust acting directly on the hull. The method of analysis for this condition is described in this section.

It is noted (reference (k)) that the lift on a body of revolution at an inclination to the airstream is composed of a part due to the potential flow and a part due to the viscous drag of the cross-flow component. At large angles of attack, the latter component is by far predominant. Also, there is some question as to what kind of potential flow pattern can develop over a body of revolution when the cross-flow may change from a maximum positive to a maximum negative value several times over the body length. Therefore, potential flow effects are neglected, and the forces on the hull are calculated on the basis of drag forces only, in the following manner:

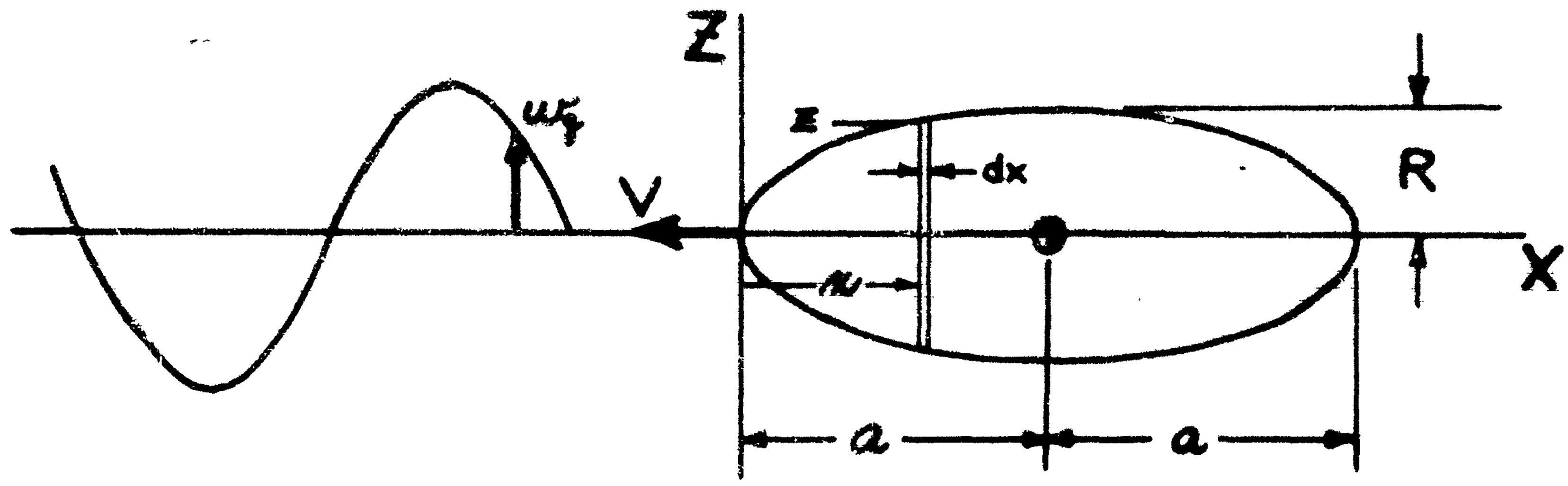

$$w_g = U \sin \frac{\pi}{2.5c}(Vt - x) \tag{B-1}$$

An alternating sinusoidal gust pattern was assumed, whose relation to the 1-cosine gust shape is shown at the right. The fin response to a 2.5-chord half sine wave is essentially the same as the response to a 3-chord 1-cosine wave form. (This relationship was chosen on the same basis as the 25-chord, 1-cosine gust shape was selected for airplanes as equivalent to the former concept of a

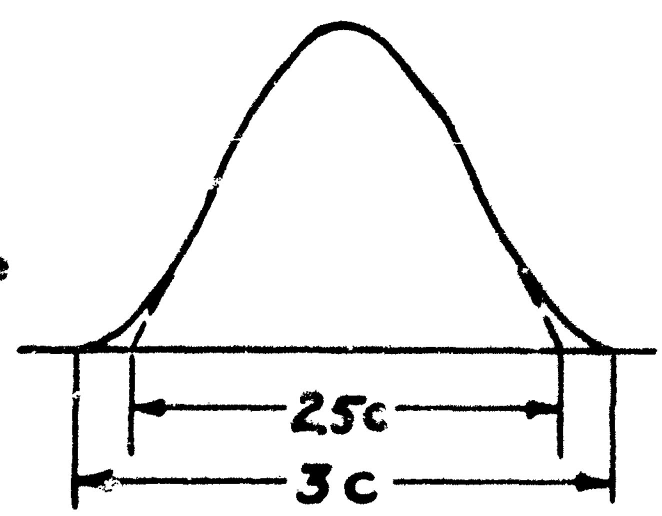

"ramp" gust shape that peaked in ten chord lengths. This point is noted in reference (a).)

Time is zero at the instant that the Z-axis, moving with the hull, is coincident with the beginning of the gust.

Consider the force acting on any slice of the hull at a distance x aft of the bow. The force on this slice is calculated on the basis of the two-dimensional viscous flow about a cylinder.

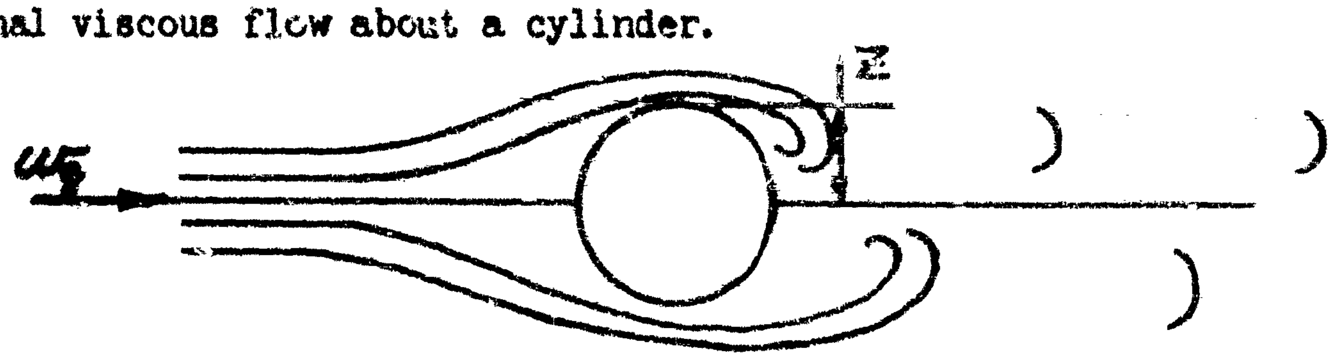

$$dF = C_d \frac{1}{2} \rho w_g^2 (2z) dx \tag{B-2}$$

In this analysis, a value of 0.5 was used for C_d, based on data given in reference (n) for the large Reynolds' Number applicable to airships. Equation (B-1) gives the value of w_g, varying with time, that acts on the slice. Assuming an elliptical hull shape,

$$z = R\left[1 - \left(\frac{x}{a} - 1\right)^2\right]^{1/2} \tag{B-3}$$

Assuming the hull c.g. to be at the center of the ellipse, the moment due to the force acting on the slice is,

$$dM = (a - x) dF \tag{B-4}$$

Combining equations (B-1), (B-2), (B-3), and (B-4) gives,

$$dM = (a-x) C_d \rho U^2 \left[\sin \frac{\pi}{2.5c}(vt-x)\right]^2 R\left[1 - \left(\frac{x}{a} - 1\right)^2\right]^{1/2} dx \tag{B-5}$$

The total moment acting at any time depends on how far the hull has penetrated into the gust, this distance being Vt. Equation (B-5) must therefore be integrated from 0 to Vt to obtain the instantaneous value of total moment. Dividing by the moment of inertia gives the rotational acceleration, from which rotational displacement can be obtained by a double integration over time.

$$\ddot{\theta} = \frac{C_d \rho U^2 R}{(1+k')I}\int_0^{Vt}\left[1-\left(\frac{x}{a}-1\right)^2\right]^{1/2}\left[\sin\frac{\pi}{2.5c}(vt-x)\right]^2\left[a-x\right]dx \tag{B-6}$$

This integral can be put in terms of the dimensionless parameter x/a by changing equation (B-6) to:

$$\ddot{\theta} = \frac{C_d \rho U^2 R a^2}{(1+k')I}\int_0^{Vt/a}\left[1-\left(\frac{x}{a}-1\right)^2\right]^{1/2}\left[\sin\frac{\pi a}{2.5c}\cdot\frac{vt-x}{a}\right]^2\left[1-\frac{x}{a}\right]d\left(\frac{x}{a}\right) \tag{B-7}$$

All the terms inside the integral are independent of the geometry of the airship except for the ratio a/2.5c, which relates the hull length to the length of gust critical for the fin. Typical values of a/c, the ratio of hull length to fin chord, are:

ZS2G-1:	2.84
ZSG-4:	3.73
ZPG-2:	3.72
ZR-3:	4.82

These values do not cover too wide a range to prevent choosing one representative value of a/2.5c as generally applicable to all airships. It must be remembered that the critical lengths of gusts had a broad range (note Figure 5) and the one selected for analysis (represented here by 2.5) was fairly arbitrary. If longer gusts are taken in combination with airships having a higher value of a/c, the value a/2.5c = 3/2.5 can be considered reasonably applicable to all airships. Solutions for any airship, therefore, can be obtained by using appropriate values for the constants outside the intergral.

Solutions obtained for the ZS2G-1 airship are shown in Figure 7.

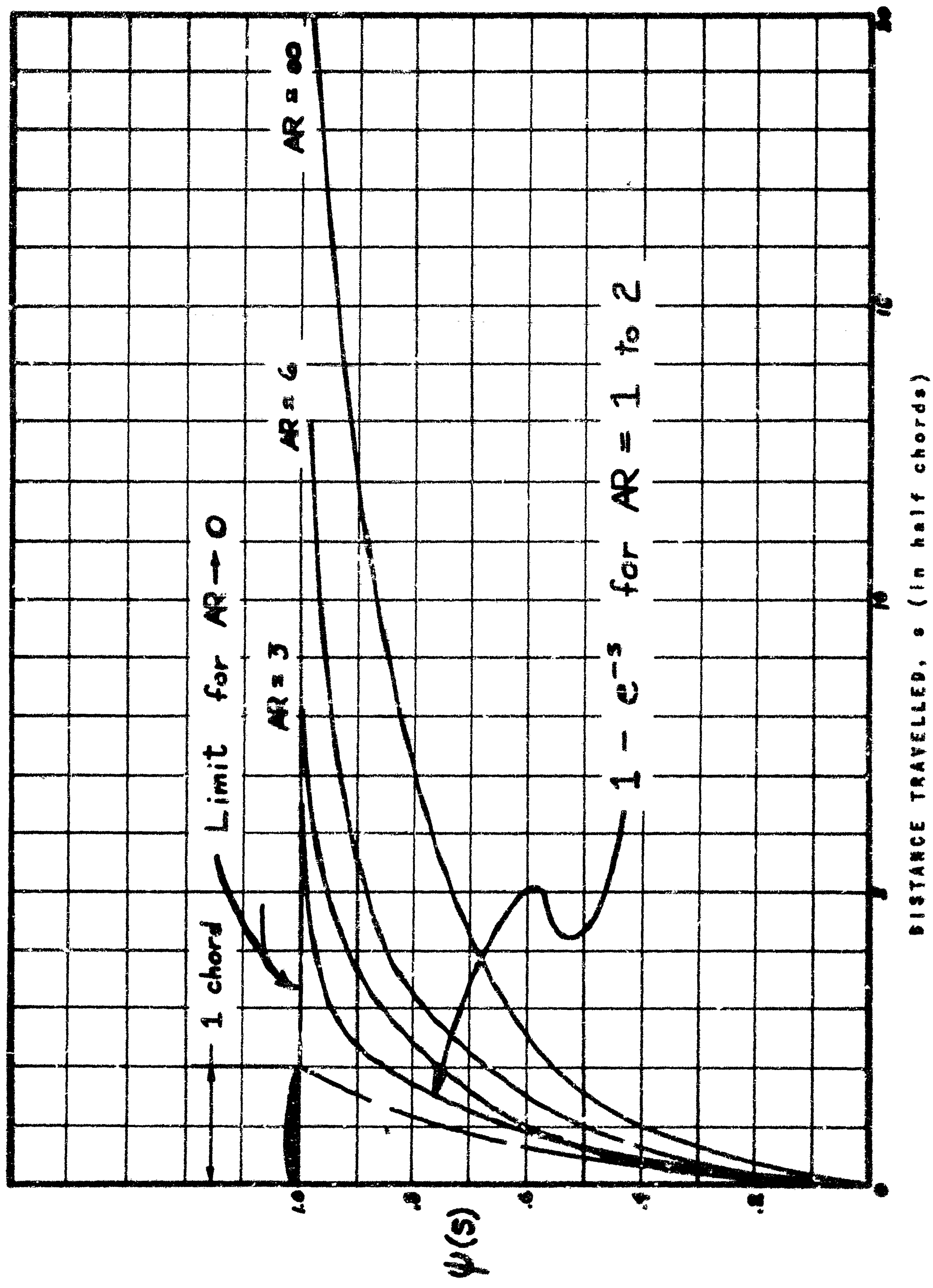

LIFT-LAG FUNCTIONS

FIG. 1

McLEAN *Development Laboratories, Inc.*

Contract No. NOrd 56-795-c

Report No. E-114

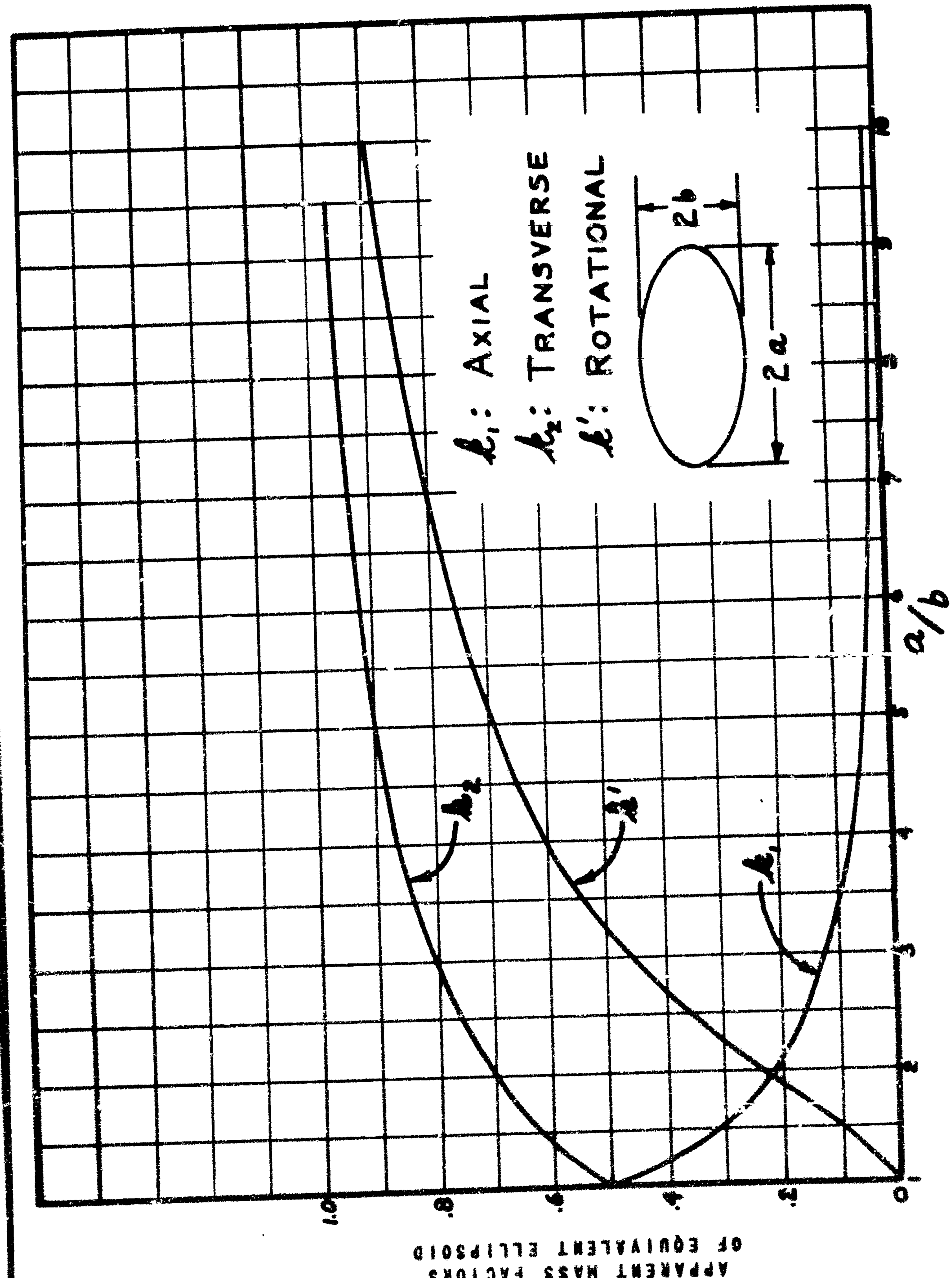

APPARENT MASS FACTORS

FIG. 2

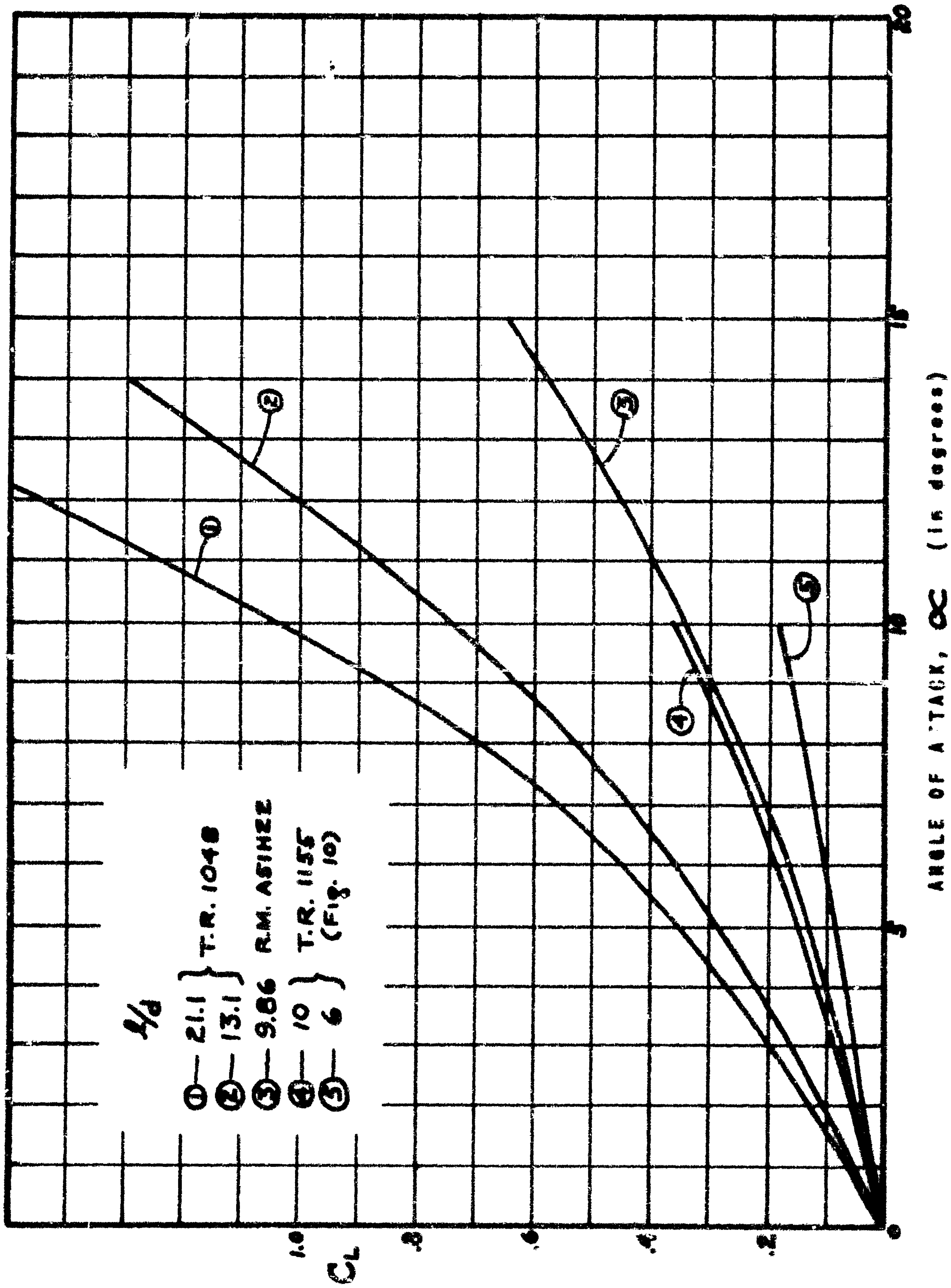

FIG. 3 LIFT COEFFICIENTS OF BODIES OF REVOLUTION

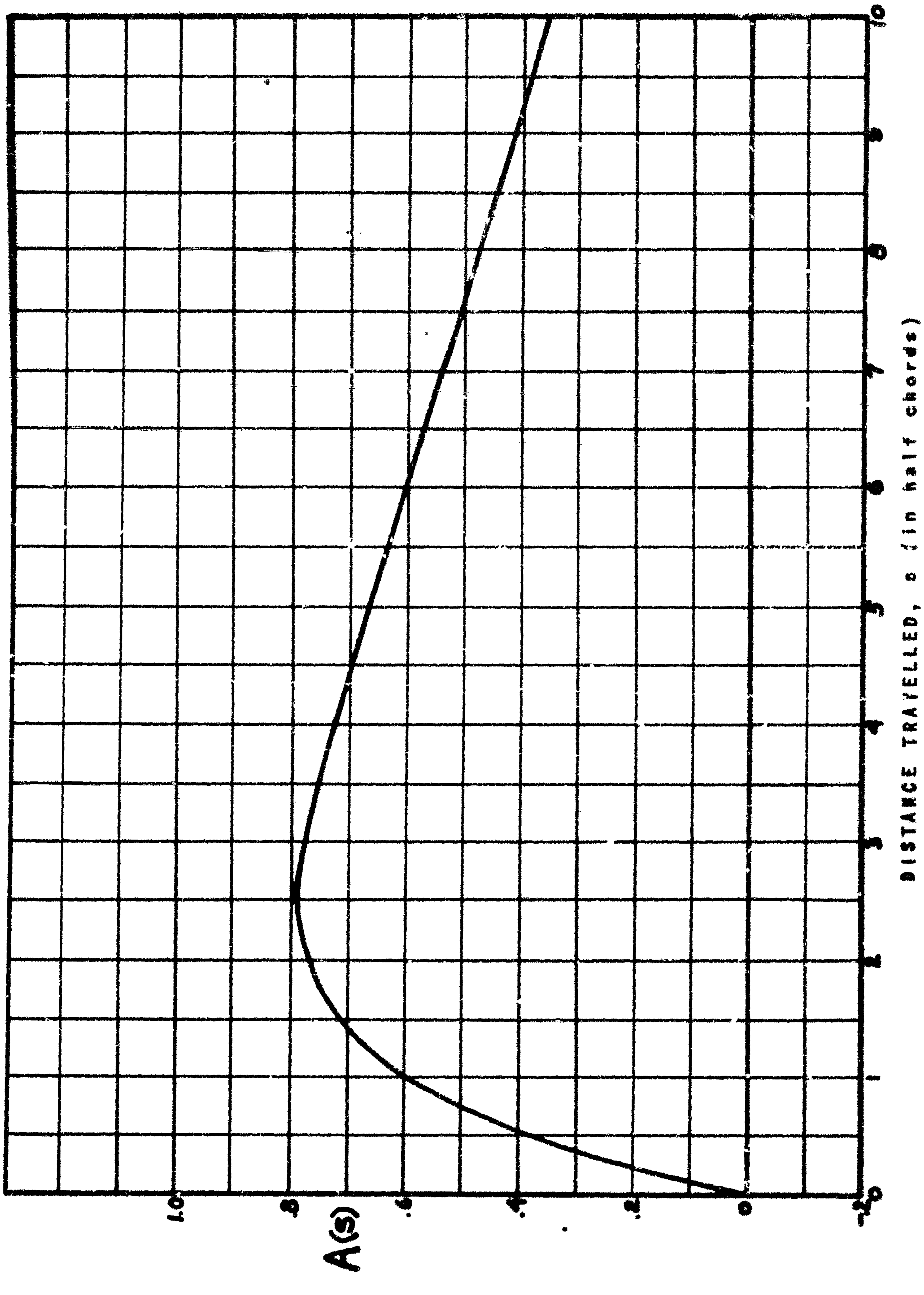

FIG. 4 ZSG-4 RESPONSE TO SHARP-EDGE GUST

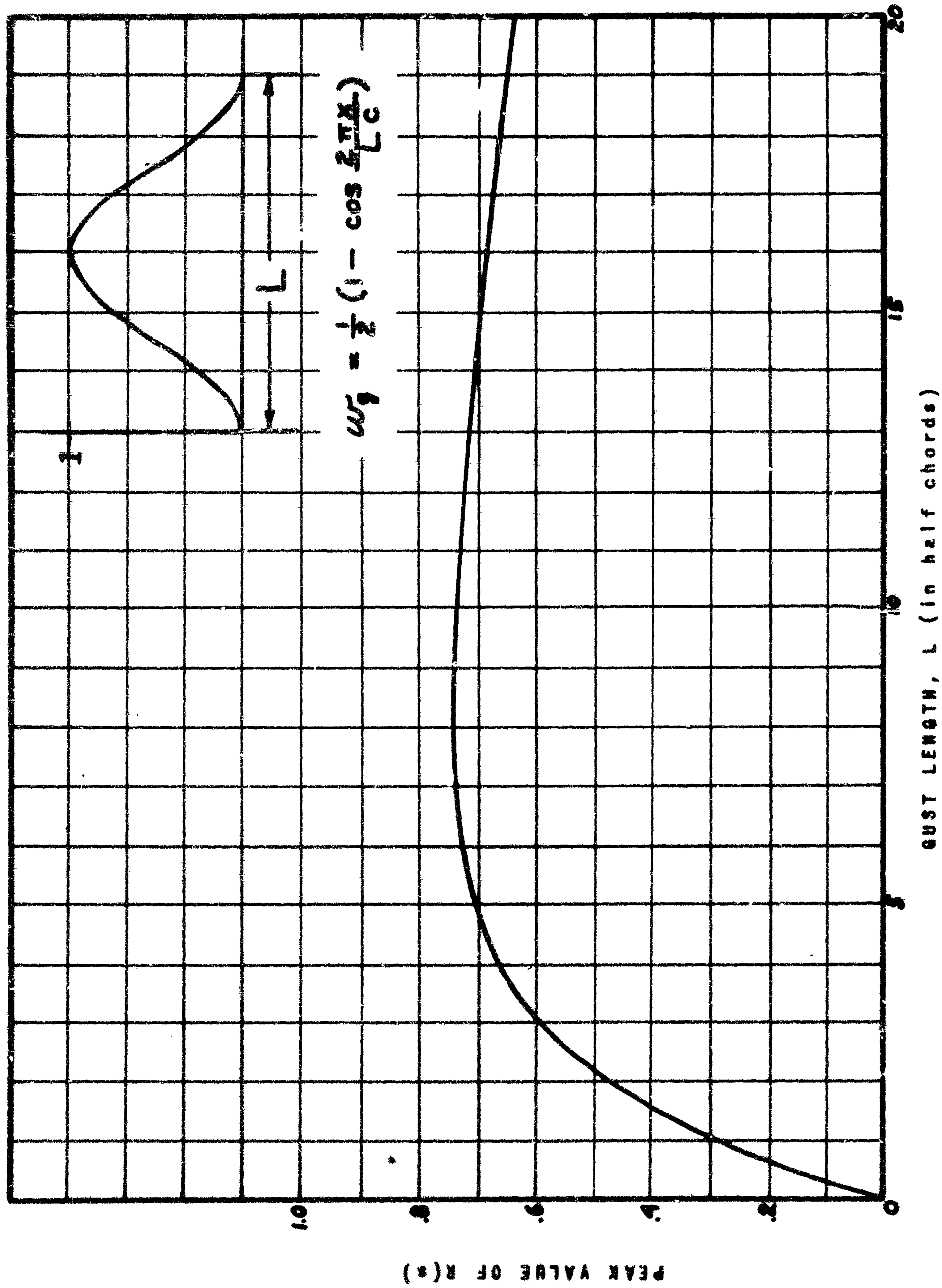

FIG.5 ZSG-4 PEAK RESPONSE TO GUSTS OF VARIOUS LENGTHS

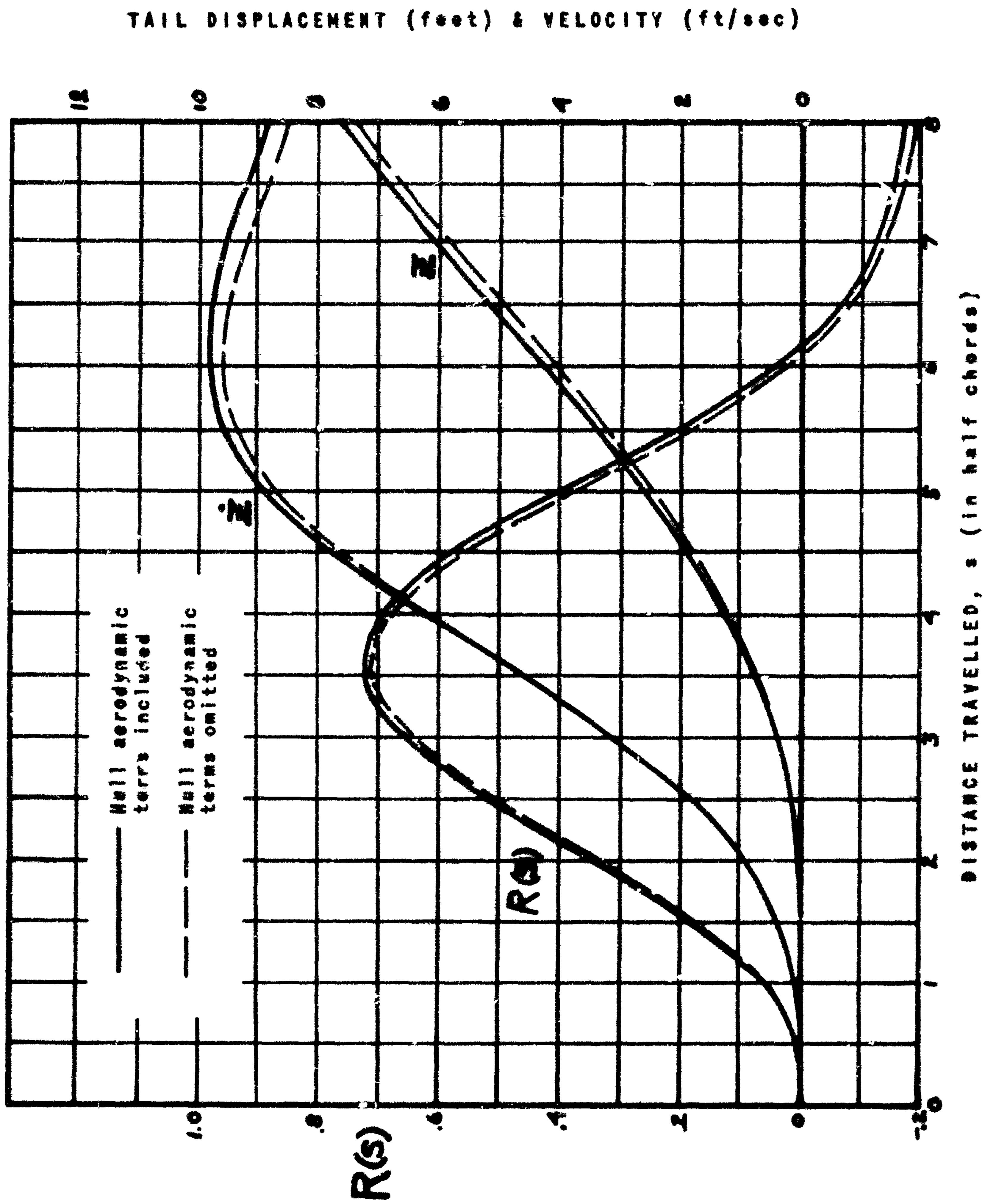

FIG. 6 ZSG-4 RESPONSE TO 3-CHORD-LENGTH GUST

McLEAN Development Laboratories, Inc.

Contract No. NOas 56-795-c Report No. E-114

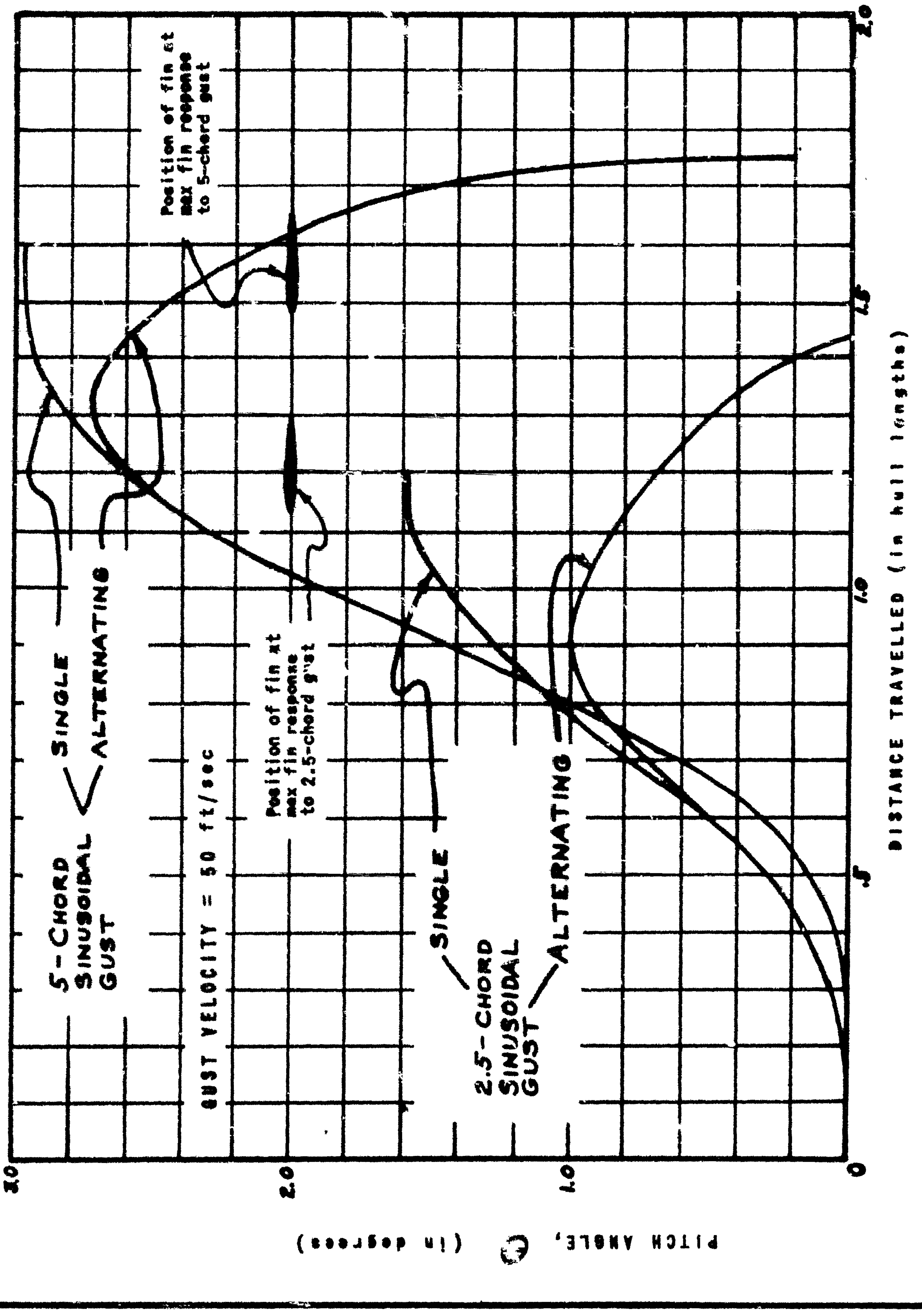

FIG. 7 ZS2G-1 PITCHING CAUSED BY GUST ACTING ON HULL

Contract No. NOas 56-795-c

Report No. E-114

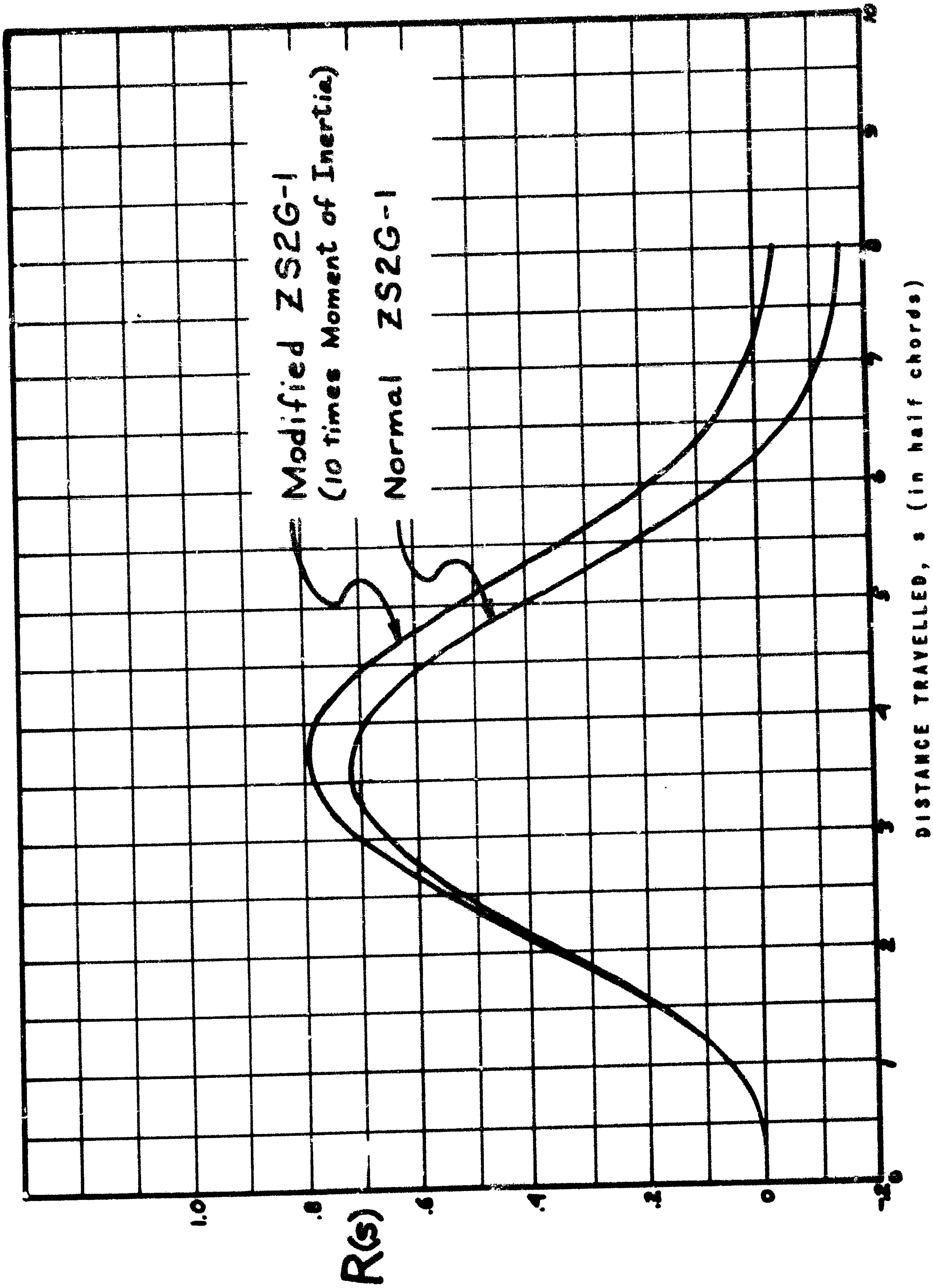

FIG. 8 TIME HISTORIES OF MODIFIED ZS2G-1

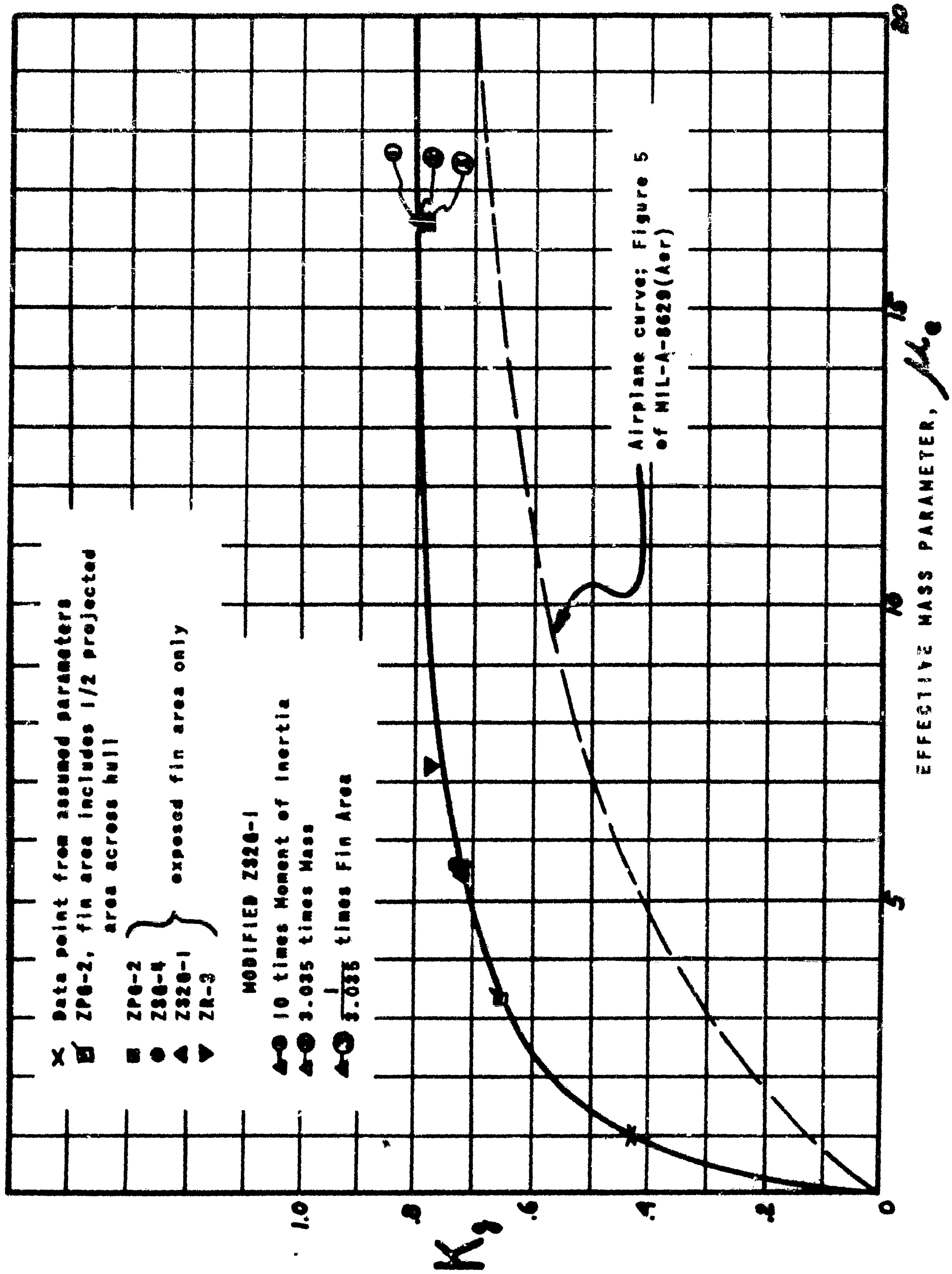

FIG. 9 GUST FACTOR VERSUS EFFECTIVE MASS PARAMETER